Article

Cell Press

Insulin Receptor-Related Receptor as an Extracellular Alkali Sensor

Igor E. Deyev,[1] Fabien Sohet,[4,5] Konstantin P. Vassilenko,[6] Oxana V. Serova,[1] Nadezhda V. Popova,[1] Sergey A. Zozulya,[1] Elena B. Burova,[6] Pascal Houillier,[4,5,7] Dmitry I. Rzhevsky,[2] Anastasiya A. Berchatova,[2] Arkady N. Murashev,[2] Anton O. Chugunov,[3] Roman G. Efremov,[3] Nikolai N. Nikol'sky,[6] Eugenio Bertelli,[8] Dominique Eladari,[4,5,7] and Alexander G. Petrenko[1,*]

[1]Laboratory of Receptor Cell Biology
[2]Biological Testing Laboratory
[3]Laboratory of Biomolecular Modeling
Shemyakin-Ovchinnikov Institute of Bioorganic Chemistry, Russian Academy of Sciences, Moscow 117997, Russia
[4]Université Paris Descartes, Institut National de la Santé et de la Recherche Médicale UMRS 872, Equipe 3,
and Centre de Recherche des Cordeliers
[5]Université Pierre et Marie Curie and Centre National de la Recherche Scientifique ERL7226
15 Rue de l'Ecole de Médecine, F-75006, Paris, France
[6]Department of Intracellular Signaling and Transport, Institute of Cytology, Russian Academy of Sciences, Saint Petersburg 194064, Russia
[7]Hopital Européen Georges Pompidou, Département de Physiologie, Assistance Publique-Hopitaux de Paris, 20 rue Leblanc, F-75015, Paris, France
[8]Department of Physiopathology, Experimental Medicine and Public Health, University of Siena, 53100 Siena, Italy
*Correspondence: petrenkoag@gmail.com
DOI 10.1016/j.cmet.2011.03.022

SUMMARY

The insulin receptor-related receptor (IRR), an orphan receptor tyrosine kinase of the insulin receptor family, can be activated by alkaline media both in vitro and in vivo at pH >7.9. The alkali-sensing property of IRR is conserved in frog, mouse, and human. IRR activation is specific, dose-dependent and quickly reversible and demonstrates positive cooperativity. It also triggers receptor conformational changes and elicits intracellular signaling. The pH sensitivity of IRR is primarily defined by its L1F extracellular domains. IRR is predominantly expressed in organs that come in contact with mildly alkaline media. In particular, IRR is expressed in the cell subsets of the kidney that secrete bicarbonate into urine. Disruption of *IRR* in mice impairs the renal response to alkali loading attested by development of metabolic alkalosis and decreased urinary bicarbonate excretion in response to this challenge. We therefore postulate that IRR is an alkali sensor that functions in the kidney to manage metabolic bicarbonate excess.

INTRODUCTION

Insulin receptor-related receptor (IRR) is a member of the family of three structurally related receptor tyrosine kinases that includes insulin receptor (IR) and insulin-like growth factor receptor (IGF-IR) (Shier and Watt, 1989; Ullrich et al., 1985, 1986). Natural agonists of the latter two are insulin and two insulin-like growth factors, IGF-I and IGF-II. While stimulation of IR with insulin primarily modulates cellular metabolism, the main function of activated IGF-IR is to promote cell proliferation and survival (De Meyts, 2002; Dupont and LeRoith, 2001). Although insulin binds to IR with approximately 100-fold higher binding affinity as compared to IGF-IR, it can also stimulate the latter at higher concentrations; the same is true for IGF-I and IR. In contrast, none of the known IR or IGF-IR ligands can activate IRR (Jui et al., 1994; Zhang and Roth, 1992), and the physiological role of IRR has remained enigmatic primarily because no endogenous ligands for IRR have been identified since its discovery in 1989, despite significant efforts that included the genome analysis (Dissen et al., 2005).

Contrary to the widespread distribution of IR and IGF-IR in different tissues and cell types, IRR is primarily expressed in the kidneys, stomach, and pancreas (Hirayama et al., 1999; Mathi et al., 1995)—organs that exhibit acid or base-transporting epithelia. Chimeric receptors with IRR intracellular signaling domain, fused to other activatable receptors' ectodomains, can signal via insulin-similar pathways that involve insulin receptor substrate-1 (IRS-1) and IRS-2 (Hirayama et al., 1999), as well as GAP-associated p60 and Shc, and results in the stimulation of glucose uptake (Dandekar et al., 1998). Also, chimeras of IRR with BDNF receptor can promote neuronal survival and PC12 cells differentiation (Kelly-Spratt et al., 1999; Kelly-Spratt et al., 2002). Yet, the signaling properties of the IRR kinase domain were found to differ significantly from those of IR and IGF-IR (Klammt et al., 2005).

No overt phenotype under normal conditions was detected in mice with targeted inactivation of the IRR gene (Kitamura et al., 2001), while the triple-knockout of IRR, IR, and IGF-IR revealed a redundant role of all three receptors in male gonad development (Nef et al., 2003) that has not received any mechanistic explanation. The phylogenetic analysis of the IRR orthologous sequences indicated that IRR, as a separate entity from IR and IGF-IR, evolved in amphibians and remained conserved in
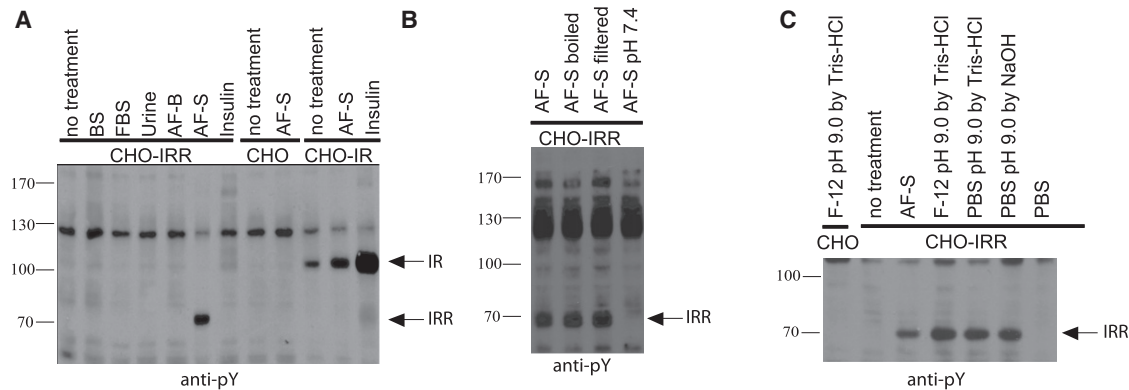
Figure 1. Activation of IRR in Transfected Cells
(A) Fluids stimulation of tyrosine phosphorylation in CHO-IR and CHO-IRR cells. The starved cells were incubated with 10% of the indicated fluids or 1 μM insulin in F-12 media for 10 min, lysed and analyzed by western blotting with anti-pY antibody. BS, bovine serum; FBS, fetal bovine serum; AF-B, bovine amniotic fluid (Biolot, Russia); AF-S, bovine amniotic fluid (Sigma); PBS, phosphate-buffered saline.
(B) Characteristics of the IRR activation. The sample of amniotic fluid was boiled for 5 min, or filtered through a 1000 Da cutoff membrane, or adjusted to pH 7.4 with Tris-HCl and tested as in (A).
(C) Stimulation of CHO-IRR cells with alkaline media. The CHO and CHO-IRR cells were incubated for 10 min with the indicated media and analyzed as in (A). All western blots shown are representative of at least three independent experiments.

mammals. It also revealed a strong selective pressure, suggesting an as yet unknown important function of IRR (Hernández-Sánchez et al., 2008; Rentería et al., 2008).

To get an insight into the function of IRR, we embarked on a search for endogenous agonist of this receptor. We determined that IRR activation could be achieved by a sole increase in the extracellular pH value. IRR activation by alkaline media was specific, dose dependent, reversible, determined by the receptor ectodomain, and accompanied by a conformational change of the receptor molecule, thus resembling typical features of the ligand-receptor interaction. It also triggered the intracellular signaling that involved IRS-1 and AKT/PKB and involved actin cytoskeleton remodeling. The analysis of $IRR^{-/-}$ mice revealed an impaired renal response to alkali loading attested by decreased urinary bicarbonate excretion and development of metabolic alkalosis in response to this challenge. Our data suggest a role of IRR as a cell-surface alkali-sensing receptor that is involved in renal adaptation to metabolic alkalosis.

RESULTS

IRR Activation by Alkaline Media
Since IRR is primarily found in kidney epithelial cells, we tested several physiological liquids that may come in contact with them, including normal and fetal serum, urine, and amniotic fluid, for their ability to stimulate receptor autophosphorylation in cell lines stably transfected with hemagglutinin (HA)-tagged human IRR, and also with IR or IGF-IR as controls. Among several samples analyzed, commercially available amniotic fluid AF-S produced strong and reproducible tyrosine phosphorylation of a protein species corresponding to the size of the phosphorylated IRR β subunit. In IR-expressing cells, insulin produced strong stimulation, whereas amniotic fluid treatment showed only a minor, if any, effect that could result from endogenous insulin in this fluid (Figure 1A). The stimulatory activity of amniotic fluid was resistant to heat denaturing and was permeable

through regular or 1000 Da cutoff dialysis membranes, but sensitive to mild acidification. Neutralization of the amniotic fluid sample by adjustment to pH 7.4 completely eliminated the IRR response (Figure 1B).

We noted that, among the biological fluids tested, only the AF-S samples of amniotic fluid had pH of about 8.5-9.0, other fluids being neutral or mildly acidic. We therefore tested whether alkaline media, per se, may be the cause of IRR activation. It appeared that a regular cell conditioned medium, adjusted to pH 9, produced robust stimulatory effect in IRR-expressing cells, whereas neutral media did not produce any response (Figure 1C). Hence, we hypothesized that IRR acts as an alkaline pH sensing receptor.

Preliminary experiments indicated that pH sensitivity of overexpressed IRR was detected in all cell lines tested (Figures 1C, 2A, and 2B and Figure S1A available online). When the transfected cells were exposed to alkaline media for 50 min, followed by IRR immunoprecipitation and western blotting with anti-pY antibody, a reliably detectable IRR response was already observed at pH 7.9 (Figure 2B and Figure S1B).

Since IRR evolved in amphibians, we tested whether an IRR ortholog from the most distant species also had the alkaline-sensing property. The complementary DNA (cDNA) of *Xenopus laevis* IRR was expressed as HA-tagged protein in HEK293 cells, and the cells were treated with alkaline media or with insulin. Immunoprecipitation revealed robust activation of the receptor as a result of the treatment with alkali, whereas no response to insulin could be detected (Figure 2C).

We also checked whether endogenous IRR in its native environment would retain its pH responsiveness. We treated with alkaline media mouse MIN6 insulinoma cells that were shown to express IRR (Hirayama et al., 1999). The cell lysates were immunoprecipitated with anti-IRR antibody. Western blotting of the precipitates with antiphosphotyrosine antibody revealed IRR activation only in the sample incubated with the alkaline medium (Figure 2D).
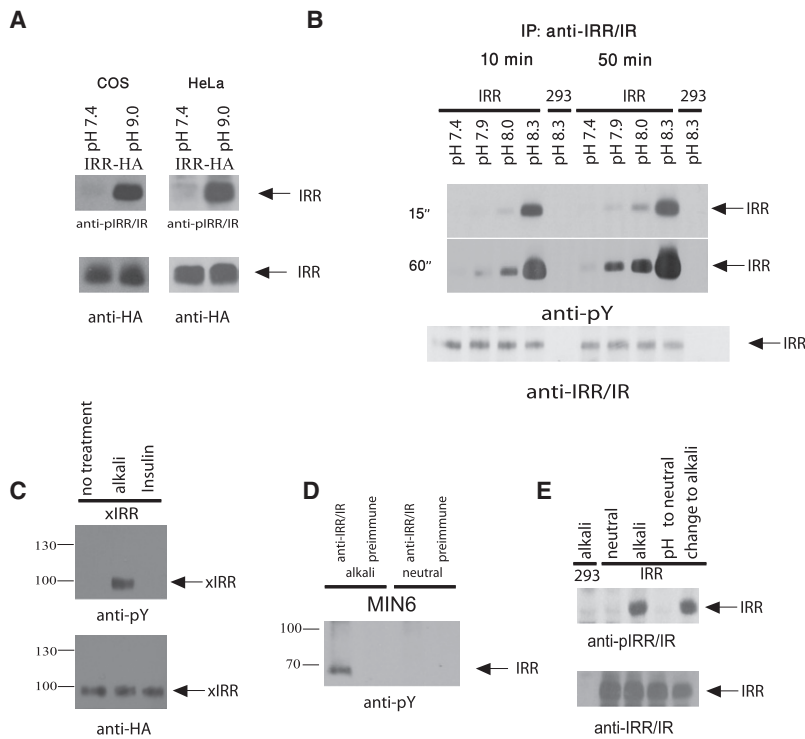
A

COS   HeLa

B

IP: anti-IRR/IR

10 min   50 min

C

D

E

Figure 2. IRR Can Be Activated by Mildly Alkaline Media

(A) COS and HeLa cells, transfected with IRR, were treated with neutral and alkaline media and then lysed and blotted with anti-pIRR/IR or anti-HA antibodies.

(B) IRR-transfected HEK293 cells were incubated for 10 or 50 min in PBS media, adjusted to the indicated pH with 60 mM EPPS; the cells were then lysed, immunoprecipitated with anti-IRR/IR antibodies, and blotted with anti-pY (two ECL exposure times of the same blot are shown on the left) or anti-IRR/IR antibodies. Semiquantitative densitometry is shown on Figure S1B.

(C) Activation of IRR from *Xenopus laevis* (xIRR) by alkali. HEK293 cells were transfected with xIRR expression plasmid. After starvation, cells were incubated for 10 min in PBS and adjusted to pH 9.0 by Tris-HCl or with 1 μM insulin. The cells were then lysed and immunoprecipitated with anti-HA-agarose. The precipitates were stained with anti-pY or anti-HA antibodies. β subunit bands are indicated by arrows.

(D) Activation of endogenous IRR in MIN6 cells. Serum-starved MIN6 cells were incubated for 10 min in PBS pH 7.4 or PBS adjusted to pH 9.0. The cells were lysed and immunoprecipitated with anti-IRR/IR antibody or preimmune serum and blotted with anti-pY antibody.

(E) Reversibility of IRR activation after extensive washes. HEK293 cells transfected with IRR were incubated with PBS pH 9.0 and then washed extensively with PBS pH 7.4 and treated again with PBS pH 9.0 (see the Supplemental Experimental Procedures for details). Cell lysates were blotted with anti-pIRR/IR and anti-IRR/IR antibodies.

All western blots shown are representative of at least three independent experiments. See also Figure S1.

Does IRR activation by alkaline media involve any peptide or protein ligand? Contrary to IR, no basal phosphorylation of IRR was detected in cells, independently of prior starvation, suggesting the absence of endogenous IRR agonists in the serum-containing cell conditioned media (Figure S1A). We next tested the possibility that the alkali treatment results in secretion of IRR agonist. However, alkaline cell conditioned media, removed from the activated cells, after neutralization, did not produce any response in another fresh batch of CHO-IRR cells (Figure S1C). We also performed extensive washing of IRR-transfected cells with large volumes of neutral and alkaline PBS. IRR in the washed cells was still activated by alkaline media, thus ruling out the possibility that any soluble hormone-like substance, resembling insulin or IGF, is involved in the receptor activation (Figure 2E). In a most simple experiment, we achieved specific IRR activation by simply adding a calculated small amount of sodium hydroxide solution to cells in physiological salt solution as medium (Figure S1D). We also found that IRR remained insensitive to insulin at pH 8.3 (Figure S1E).

IRR activation by a pH change rather than a peptide or protein molecule should be quickly and fully reversible because it does not involve slow-kinetics dissociation of a ligand typically bound by multipoint interactions. To test this assumption, we sequentially treated IRR-expressing cells with alkaline and neutral media. This experiment revealed that, indeed, IRR can be quickly (less than 1 min) dephosphorylated upon neutralization (Figure S1F). When the neutralized cells were further treated with the alkaline medium, IRR was activated again to the same extent (Figure 2E). To determine whether protein tyrosine phosphatases

were involved in IRR desensitization, we treated the cells bearing activated IRR with pervanadate prior to neutralization. This treatment abolished IRR dephosphorylation, thus indicating the phosphatase engagement (Figure S1G).

Specificity of IRR Activation by Alkali

The receptor activation by alkali was specific for IRR as compared to other receptor-like tyrosine kinases. Whereas insulin produced a strong autophosphorylation response in IR and a weaker one in IGF-IR (Figure 3A, central and right sections), but not in IRR (Figure 3A, left section), alkalinization resulted in the activation only of IRR, but not of IR, IGF-IR, or the epidermal growth factor receptor (Figure S2A). Unlike nonspecific activation of cellular tyrosine kinases by high-salt buffers, alkali treatment produced a noticeable increase in tyrosine phosphorylation of the IRR but not of other endogenous phosphoproteins (Figure S2B).

It has been shown that insulin binding to IR results in a major conformational change of the receptor. This change could be monitored by the analysis of receptor hydrophobicity in the detergent phase distribution assay (Flörke et al., 2001). We analyzed the distribution of HA-tagged IR, IRR, and their ectodomain chimera IRR/IR between aqueous and detergent phases induced by warming Triton X-114 extracts of the transfected cells as a function of insulin or alkali addition (Figure 3B and Figure S2C). Insulin binding to IR resulted in a major shift of the ligand-receptor complexes from the detergent (lower) to the aqueous (upper) phase. No change in IRR or IRR/IR distribution was observed upon insulin addition. On the contrary, the
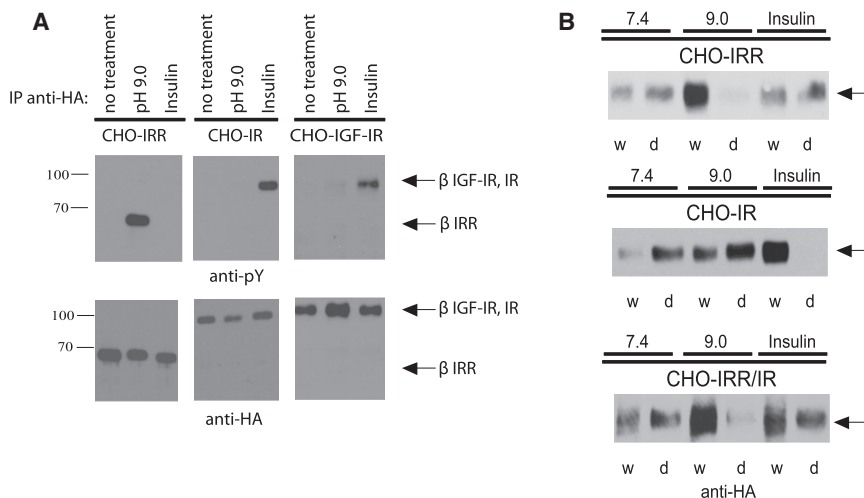
Figure 3. Specificity and Structural Response to IRR Activation by Alkali
(A) Activation of IRR but not of IR and IGF-IR by alkali. After starvation, the indicated stably transfected cell lines were incubated for 10 min in PBS adjusted to pH 9.0 or with 1 μM insulin. Cells were then lysed, immunoprecipitated with anti-HA antibody, and western blotted with anti-pY or anti-HA antibody.
(B) Analysis of IRR, IR, and IRR/IR chimera conformational changes by the detergent phase distribution assay. Nonstarved stably transfected CHO cells were lysed in Triton X-114 containing buffers adjusted to pH 7.4 or 9.0, or supplemented with 0.5 μM insulin, and analyzed by detergent phase distribution (Flörke et al., 2001), as described in detail in the Supplemental Experimental Procedures. Equal aliquots of the separated phases (w, detergent-depleted; d, detergent enriched) were western blotted with anti-HA antibody to determine receptor concentration.
See also Figure S2.

adjustment of the extracts pH to 9 induced the transfer of both IRR and IRR/IR to the upper phase without a noticeable effect on the IR distribution. We may therefore conclude that the pH increase induces a conformational change of IRR which is determined by its ectodomain and is essentially similar to the rearrangement of IR that follows the insulin binding.

pH Dependence and Positive Cooperativity of IRR Activation

We observed activation of IRR from pH 7.9 and up to pH 10.5 (Figure S3A), while no activation could be detected by acidic media at pH 5.0 to 7.4 (Figure S3B). To analyze the pH dependence of IRR response in detail, we incubated IRR-expressing cells with a set of Tris-buffered physiological saline solutions with variable pH from 7.4 to 9.2 in small increments. Cell lysates were directly analyzed by western blotting with anti-phosphoIRR antibody (Figure 4A). For semiquantitative evaluation, the blots were scanned, and the ratio of integral density of the phosphoIRR to the HA bands was plotted versus pH. The resulting plot showed a sigmoid-shaped sharp response with half effect at pH 8.4 and saturation at about pH 9.0–9.2 (Figure 4B). Interestingly, the activation showed strong positive cooperativity (Hill coefficient 3.5 ± 0.5, calculated by GraphPad Software) in contrast with IR activation by insulin that shows negative coop-

erativity (De Meyts, 2008). Apparently, the structural mechanisms of IRR activation are different from the activation of IR that involves the simultaneous interaction of the insulin molecule with two receptor subunits (De Meyts, 2008).

Structural Characteristics of IRR Activation

To analyze the mechanism of the observed IRR phosphorylation, we prepared two sets of mutants with altered extracellular and intracellular domains of the receptor. As previously reported, mutations of tyrosines 1118 and 1119 at the kinase active site of TrkB/IRR chimera abolished BDNF-induced autophosphorylation and the downstream signaling (Kelly-Spratt et al., 1999). We prepared a similar point mutant of IRR (Figure 5A, left panel). No tyrosine phosphorylation of the mutant was observed upon alkali treatment (Figure 5A, right panel) suggesting that the observed effect was due to autophosphorylation of IRR.

To determine the role of IRR ectodomain in its phosphorylation, we prepared a set of IRR/IR chimeras (Figure 5B, left panel). The first one contained the entire extracellular region of IRR fused with the rest of IR (IRR/IR). The other constructs were made by partial swapping of the extracellular regions of IRR and IR, according to their domain structure. Different combinations of L1, F, and L2 domains of IR were replaced with those of IRR (constructs IRR_L1FL2/IR, IRR_L1F/IR, and IRR_L2/IR).
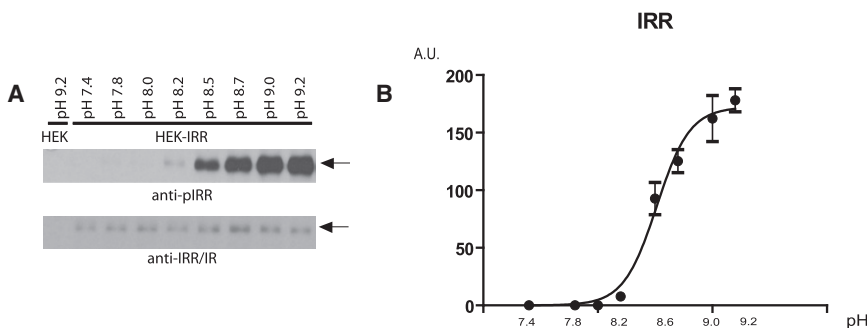

Figure 4. pH Dependence of IRR Activation
(A) Nonstarved IRR-transfected HEK293 cells were incubated for 10 min with PBS medium adjusted to the indicated pH by 60 mM Tris-HCl buffer and then lysed and blotted with anti-pIRR/IR and anti-IRR/IR antibodies. Western blot images representative of four independent experiments are shown. β subunit bands are indicated by arrows.
(B) The western blot images were scanned in the area of the IRR β subunit band, and the integrated optical density of the anti-pIRR/IR images, normalized by the anti-IRR/IR density, was plotted versus the pH of the tested solutions. Values are means ± standard error (SE; n = 4).
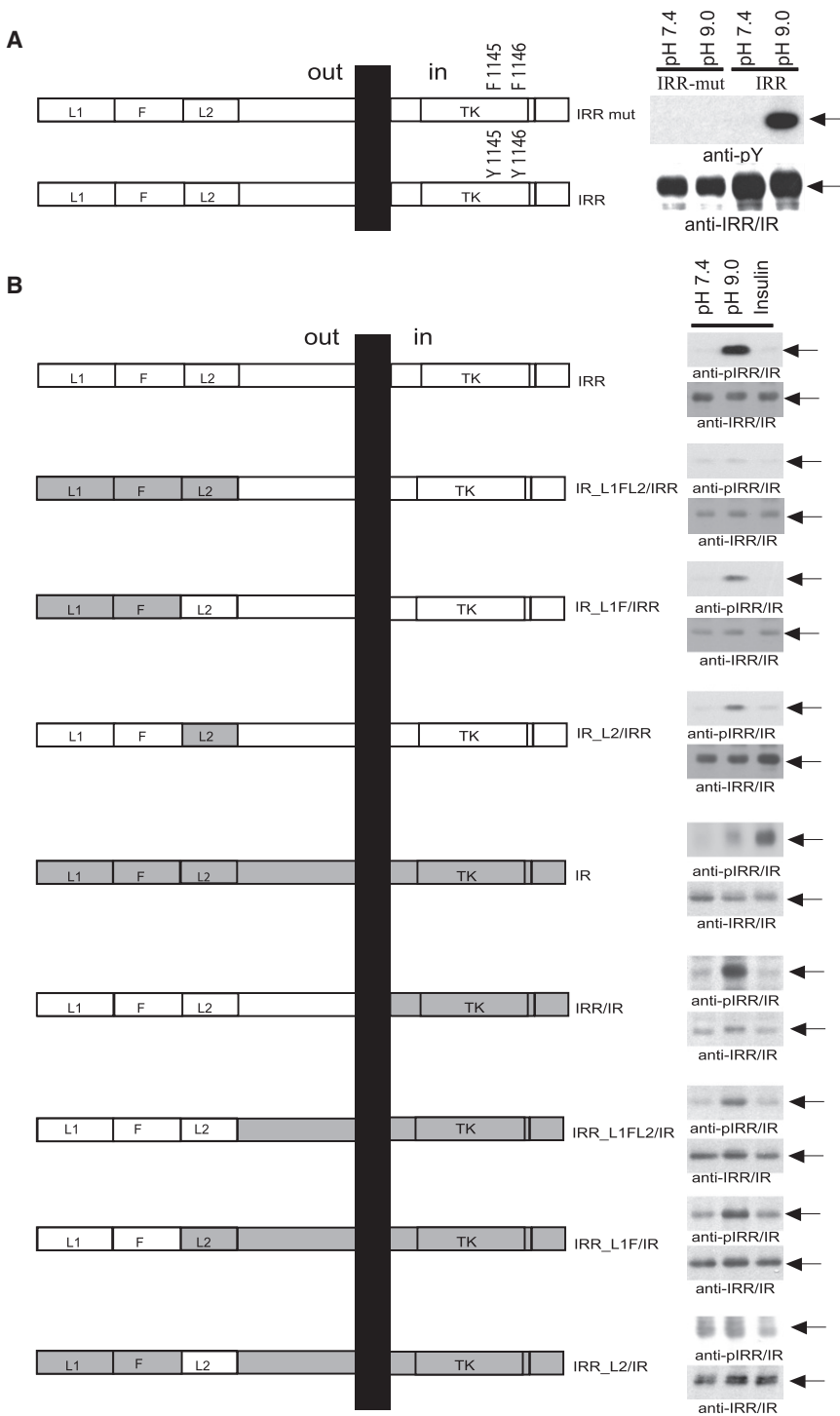See also Figure S3.

A

B

Figure 5. Structural Determinants of IRR Activation

(A) Inhibition of IRR activation by tyrosine mutations (IRR mut) in the catalytic domain (left). HEK293 cells were transfected with HA-tagged IRR and mutated IRR. After 24 hr growth, the cells were starved for 12 hr and then incubated for 10 min in PBS medium at pH 7.4 or 9.0. Cell lysates were analyzed by western blotting with anti-pY or anti-IRR/IR antibodies (right). β subunit bands are indicated by arrows.

(B) Domain models of the HA-tagged IRR/IR. L, receptor L domain; F, furin-like repeats; TK, catalytic tyrosine-kinase domain. The right panel shows activation of IRR/IR chimeras by alkali or insulin. HEK293 cells transfected with the indicated chimeras were treated with F-12 with an indicated pH (7.4 or 9.0), or supplemented with 1 μM insulin, and were then lysed and blotted with anti-pIRR/IR and anti-IRR/IR antibodies.

Arrows indicate β subunits. The western blots shown are representative of three independent experiments. See also Figure S4.

receptor response. At the same time, introduction of either L1FL2 or only L1F into IR was sufficient to render alkaline sensitivity (Figure 5B, right panels). In agreement with published work (Kristensen et al., 1999), none of the described chimeras were sensitive to insulin. We may conclude that the key residues that define IRR versus IR response are located within L1F domains. Still, other parts of IRR extracellular region are also involved to enhance the response.

To test the correct cell surface expression of these constructs, we biotinylated, lysed, and immunoprecipitated the transfected HEK293 cells with anti-IRR/IR antibody. The western blots of the precipitates, decorated with streptavidin-HRP and anti-IRR/IR antibody, revealed the appropriate presence of all constructs on the cell surface (Figure S4).

Cellular Effects of IRR Activation

We further tested whether the IRR activation by alkaline media would produce an intracellular signaling response. It was previously shown that insulin-treated chimera of IR ectodomain, fused with IRR transmembrane and intracellular regions, could

The constructs IR_L1FL2/IRR, IR_L1F/IRR, and IR_L2/IRR were prepared in an opposite manner by introducing domains of IR into IRR.

The IR/IRR ectodomain chimeras were tested for their response to alkaline media. The replacement of L1FL2 domains in IRR completely abolished receptor sensitivity to alkali. Replacement of either L1F or L2 significantly reduced the

be activated with insulin and induced intracellular phosphotyrosine signaling that resulted in insulin-like cell responses (Dandekar et al., 1998; Hirayama et al., 1999). We therefore examined the possibility of whether activation of IRR by alkali can stimulate intracellular signaling pathways similar to those of IR and IGF-IR. The phosphotyrosine staining of IRR-expressing cells, stimulated with alkali, revealed a 170 kDa polypeptide similar by its size
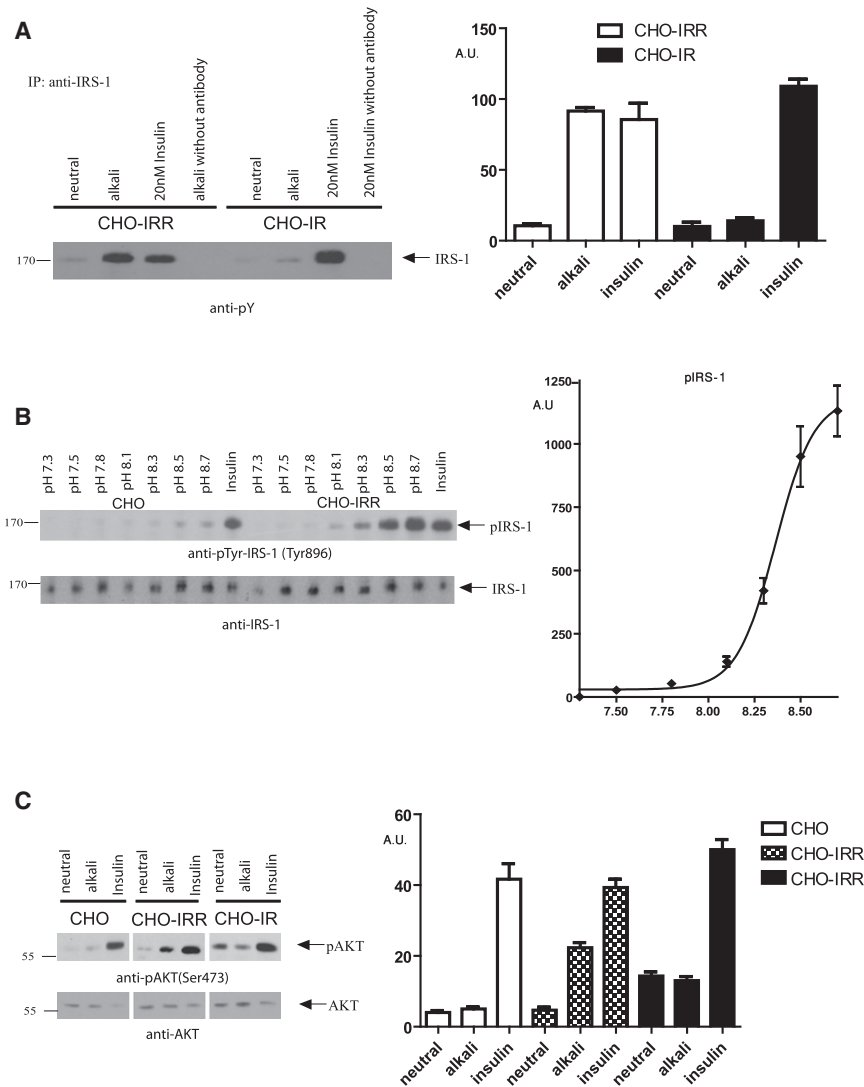
Figure 6. Intracellular Cell Signaling, Triggered by IRR Activation

(A) Phosphorylation of IRS-1 in alkali or insulin-stimulated cell lines. Nonstarved IRR and IR stably transfected cell lines were incubated for 10 min in F12 medium pH 7.4 or 9.0 and were then lysed and immunoprecipitated with anti-IRS-1 antibody. No antibody was added in the indicated samples as control. The precipitates were analyzed by western blotting with anti-pY antibody.

(B) pH dependence of IRS-1 signaling. CHO and CHO-IRR cell lines were incubated for 10 min with PBS, adjusted to the indicated pH with 60 mM EPPS, or with 20 nM insulin. The lysed cells were western blotted with anti-pIRS-1 and anti-IRS-1 antibodies.

(C) AKT signaling in alkali-stimulated cell lines. CHO, CHO-IRR, and IR cells were treated with F-12 pH 7.4, pH 9.0, or with 1 μM insulin for 10 min at 37°C. The lysed cells were blotted with anti-pAKT, or anti-AKT antibodies. Original blots representative of three independent experiments are shown on the left. Semiquantitative densitometry data as in Figure 4 are presented on the right. The data were normalized by total density (minus background) of each blot.

Values are means ± SE. See also Figure S5.

to IRS-1, and immunoprecipitation with a specific antibody confirmed the identity of this band as IRS-1 (Figure 6A). In control tests, tyrosine phosphorylation of IRS-1 was observed in cell lines activated by insulin. The pH dependence of IRS-1 activation in CHO-IRR cells was essentially similar to those of IRR with a minor response already detectable at pH 7.8–8.1 (Figure 6B). Our results appear to be in contrast with the reported absence of interaction between IRR and IRS in an in vitro binding assay (Klammt et al., 2005). However, they correlate well with the described IRS signaling triggered by IRR chimeras (Hirayama et al., 1999).

We further tested whether other components of the IR/IGF-IR signaling pathway downstream of IRS-1 such as AKT/PKB and ERK1,2 MAP protein kinases can be activated by the alkali treatment of the IRR-expressing cells. AKT phosphorylation (Figure 6C) was detected in IRR-expressing cells. Minor if any AKT phosphorylation was observed in the alkali treated IR-expressing cells that showed a robust response to insulin in a control experiment. Surprisingly, in contrast with insulin treatment, no change of ERK 1,2 basal phosphorylation level in each of three

cell lines was detected in response to alkaline stimulation (data not shown).

We also tested whether IRR activation would result in any cytoskeleton changes because insulin stimulation was shown to cause actin stress fibers breakdown and appearance of membrane ruffles (Kanzaki, 2006). The IRR-, IRR/IR-, and IR-expressing cells were treated with alkaline media or insulin and stained with phalloidin dye and anti-HA antibody to reveal the receptor presence in particular cells. We noted reorganization of actin fibers and strong blebbing in some IRR-expressing cells as a result of alkali treatment (Figure S5A). A quantitative analysis showed that alkali treatment produced more than a 3-fold increase of blebbed cells, bearing IRR. Virtually no such effect was observed in IRR/IR- and IR-expressing cells. Interestingly, insulin treatment significantly reduced the number of blebbed cells in CHO-IR and CHO-IRR/IR cell lines (Figure S5B). Thus, the IRR activation can result in cytoskeleton rearrangements, and their specific characteristics are determined by the receptor intracellular domain. While this effect may serve as a whole-cell indicator of IRR activation, it is just an illustration of a cell response and may or may not be related to the physiological role of IRR because of its overexpression in a non-natural system.

Alkali-Induced Activation of IRR in Kidney In Vivo

We next assessed whether similar phosphorylation of IRR in response to metabolic alkalosis also occurs in vivo when IRR is expressed in its natural environment. Since manipulation of

extracellular pH in the pancreas or stomach is almost impossible, we chose for this analysis the kidney as the primary organ of IRR expression. Preceding experiments in cell models demonstrated that phosphorylation of IRR is a transient phenomenon (Figure S1F). Thus, to maximize our chances to detect IRR modifications in vivo, we designed an experiment in which kidneys of a live anesthetized rat were subjected to acute experimental alkalosis by injecting sodium bicarbonate solution into renal arteries. The kidneys were removed when pH of urine reached mildly alkaline levels of approximately pH 8, typically within 10–15 min. The kidneys were immediately homogenized in a buffer with protease and phosphatase inhibitors, and a crude membrane fraction was isolated and further extracted with a mild detergent buffer. The extracts were precipitated with anti-IRR/IR or control antibodies and western blotted with anti-phosphotyrosine antibody. As control, kidneys, perfused with similar amount of PBS pH 7.4 were used. Blot staining revealed the phosphorylated band of about 66 kDa that indicated autophosphorylation of activated IRR (Figure 7A).

Kidney Function Deficiency in *IRR* Knockout Mice

The physiological relevance of IRR as an alkali sensor was then assessed by testing the effects of *IRR* gene disruption on the animal response to experimentally induced alkalosis. Wild-type and *IRR* knockout mice were given 0.28 M $NaHCO_3$ in their drinking water for 7 days, a treatment that has been shown in mice or rat to induce mild metabolic alkalosis (Sabolić et al., 1997; Wagner et al., 2002), and acid-base parameters, obtained before and after alkali loading, were compared. A control group consisted of mice, receiving NaCl 0.28 M instead of $NaHCO_3$, to match the sodium load. Figure 7B shows that $IRR^{+/+}$ mice were able to cope with the alkali load, while $IRR^{-/-}$ mice developed compensated metabolic alkalosis. No changes in blood gas parameters were observed after administration of NaCl 0.28 M (Figures S6A and S6B).

Alkali loading normally results in increased urine pH and bicarbonate excretion, both of which reaching maximal values within a few hours. Renal bicarbonate excretion depends upon the filtered load of bicarbonate (i.e., plasma $[HCO_3^-]$ × glomerular filtration rate) and also upon renal tubular absorption of bicarbonate. We reasoned that impaired renal excretion of bicarbonate might be detectable only during the initial phase of loading, and not at steady state when $IRR^{-/-}$ mice exhibit higher plasma $[HCO_3^-]$ values than controls. We therefore assessed the effects of alkali loading on urine pH and bicarbonate excretion within the first 6 hr and then 24 hr after the beginning of loading. Alkali loading induced a very rapid increase in urine pH and bicarbonate excretion in WT mice. In contrast, the initial response was clearly blunted in $IRR^{-/-}$ mice (Figure 7C). As expected, after 24 hr of loading, mice from both genotypes were already at steady state and exhibited the same alkaline urine pH values and the same bicarbonate excretion. The defect in renal bicarbonate excretion is likely to be the consequence of abnormal bicarbonate secretion and not of decreased filtration, since glomerular filtration rate per body mass in $IRR^{-/-}$ and $IRR^{+/+}$ mice was measured as identical (Figure S6C).

Renal adaptation to an alkaline-load implies an increase in bicarbonate secretion by beta intercalated (β IC) cells of the collecting duct. This adaptation is supported by increased expression of the apical Cl^-/HCO_3^- exchanger pendrin (Wagner et al., 2002). To confirm that IRR disruption affects β IC cells, we measured the abundance of pendrin and of the B1 subunit of the V-H$^+$-ATPase in the kidney cortex of alkali-loaded $IRR^{-/-}$ and WT mice by western blot. Even though $IRR^{-/-}$ mice exhibited a much more marked metabolic alkalosis after alkaline loading (Figure 7B), and hence were expected to exhibit increased pendrin and proton pump abundance, they showed ~40% decrease in both protein abundance when compared to $IRR^{+/+}$ mice, indicating that IRR disruption impairs the capability of the collecting duct to adapt to alkalosis (Figure 7D).

DISCUSSION

Our attempts to identify an endogenous ligand of IRR, a close homolog of IR and IGF-IR that both have peptide agonists, led to the unexpected observation that IRR is activated by mildly alkaline extracellular pH, a substance of a nonpeptide nature. Moreover, in vivo experiments demonstrated that IRR is required for normal adaptation of collecting duct in response to metabolic alkalosis. Thus, we propose that IRR functions as a pH sensing receptor.

The activation of IRR by hydroxyl anion resembles canonical receptor-ligand interaction. First, it is concentration dependent, with a characteristic saturation curve, and fully reversible. Second, it is specific; two closely homologous receptors IR and IGF-IR, as well as another receptor tyrosine kinase EGFR, are not activated by alkaline media. Third, the pH-sensing property of IRR is determined solely by the structure of its extracellular domain. Like with other cell surface receptors, IRR activation by alkali triggers a conformational change in the receptor molecule, stimulates intracellular signaling (involving IRS-1 and AKT/PKB), and results in cytoskeleton rearrangement. The absence of IRR basal autophosphorylation together with the estimated pH dependence of IRR activation suggest that the hydroxyl anion is possibly its only one natural agonist and the receptor remains silent within the regular homeostasis range (pH 7.2–7.6) of blood and interstitial fluid. Whereas an alkali-sensing ion channel has been described previously (Niemeyer et al., 2007), no metabotropic-type receptors with such properties have been identified yet.

All of the previously identified receptor tyrosine kinase ligands are proteins that activate the receptors by induction of their dimerization. In the unique case of the insulin receptor family the subunits are predimerized by disulfide bonds and require allosteric activation by a ligand. Three-dimensional structures of the first three domains (L1-F-L2) of IR (Lou et al., 2006) and IGF-IR (Ward et al., 2001), as well as the whole IR ectodomain structure (McKern et al., 2006), revealed possible mechanisms of insulin and IGF capture by their receptors, and also uncovered a quite unexpected Λ shape of the IR ectodomain (a.k.a. "folded-over conformation"). These structures delineated the insulin binding to two receptor sites: site 1 lying on the surface of the central β sheet of L1 domain in one of disulfide-linked monomers of the receptor, and site 2 at the junction of FnIII-1 and FnIII-2 of the opposite monomer. Yet another, symmetrical, ligand binding site that is capable of binding another insulin molecule is formed by FnIII-1/2 of the second monomer and L1 of the first one. Insulin is proposed first to interact with the
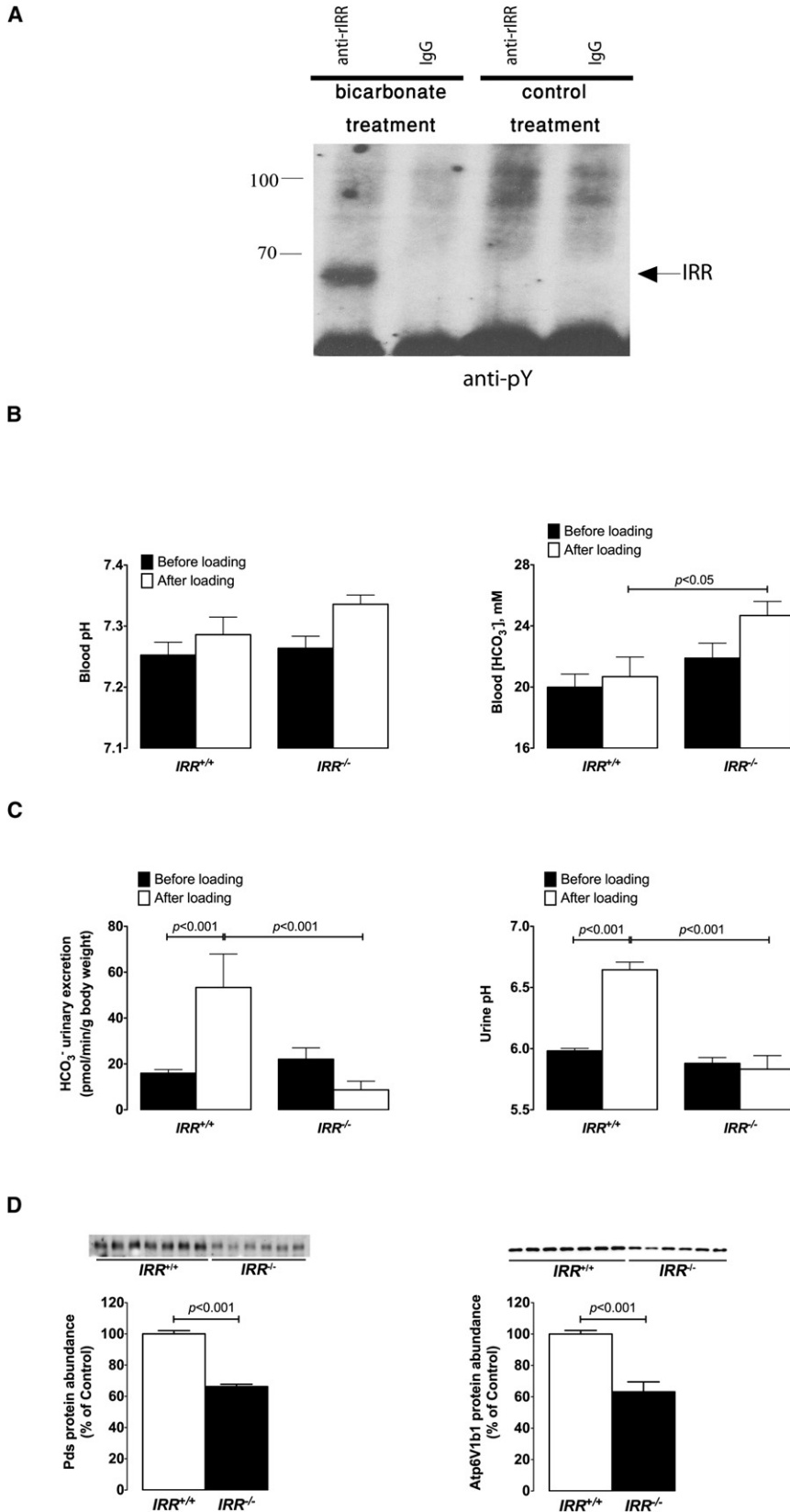
Figure 7. In Vivo Analyses of IRR Function

(A) Rats were anesthetized, and their kidneys were perfused through renal arteries with 1% solution of $NaHCO_3$ or with 0.9% NaCl (control). The kidneys were then removed and immediately homogenized and extracted, as described in the Experimental Procedures. The extracts were immunoprecipitated with affinity purified anti-rat IRR antibody or with the same concentration of rat IgGs as control and analyzed by western blotting with anti-pY antibody. The blot is representative of three independent experiments. The arrow indicates position of the IRR β subunit band.

(B) Blood gas analyses in $IRR^{+/+}$ and $IRR^{-/-}$ mice before and after 7 days of alkali load administered as 0.28 M solution of $NaHCO_3$ in the drinking water.

(C) Initial renal response to alkali loading measured in $IRR^{+/+}$ and $IRR^{-/-}$ mice. Six hour urine collections (from 9:00 a.m. to 3:00 p.m.) were obtained from same $IRR^{+/+}$ and $IRR^{-/-}$ mice administrated either dionized water on the first day of the experiment (black bars) or $NaHCO_3$ solution on the second day (white bars) to measure urine pH and renal bicarbonate excretion.

(D) Immunoblots of membrane fractions from the renal cortex obtained from $IRR^{+/+}$ and $IRR^{-/-}$ mice after 7 days of alkali loading. The membrane preparations were blotted with antibodies directed against Pds and Atp6v1b1. Densitometric analyses of data show the abundance of Pds, and Atp6v1b1, respectively, expressed as percent of control. Equality of loading was verified by running, in parallel, gels that were stained with Coomassie blue and quantified as described previously (Quentin et al., 2004a).

Values are means ± SE. See also Figure S6.

low-affinity site and then "crosslink" the receptor dimer by contacting with the second site in the opposite monomer, which creates the high-affinity site. This conformational change of the receptor is thought to be the origin of negative cooperativity (Lawrence et al., 2007), since when the primary ligand binding site is occupied, the affinity at the symmetrical site simultaneously drops (De Meyts, 2008).

Agonist of IRR—hydroxyl ion—is a small molecule and cannot exhibit simultaneous interactions with symmetrical receptor subunits like insulin does. We found that, in contrast with IR activation, IRR shows strong positive cooperativity in response to pH (Hill coefficient 3.5 ± 0.5), suggesting that several sites in the receptor molecule, primarily located in the first two domains—L1 and F—of its extracellular region, are involved in alkali sensing and react with each next hydroxyl ion more readily than the previous. Another interesting possibility to be tested is that activated IRR forms oligomers.

We can speculate that IRR pH sensitivity in 7.9–9.2 range could be determined by several amino acid residues with ionogenic groups of its ectodomain. Cysteines have close pKa about 8.5, but they presumably exist as oxidized Cys-Cys bridges within and between receptor ectodomains, as shown for homologous IR (Sparrow et al., 1997), but perhaps deserving additional tests in the case of IRR. The role of other amino acid residues such as histidines (pKa 6.5), tyrosines (pKa 10), lysines (pKa 10), and even arginines (pKa 12) is quite possible since protein microenvironment may significantly alter amino acid residue pKa values (Srivastava et al., 2007).

The proposed physiological role of IRR as a pH sensor correlates well with the known pattern of IRR distribution. In our in vitro experiments, robust phosphorylation of IRR was detectable at pH 7.9, a value that exceeds the general physiological range. However, the tissues that harbor IRR are characteristic for direct contacts with extracorporal media of extreme pH. Largest concentrations of IRR are found in the kidney where it is restricted to B type intercalated tubular cells (β IC) (Bates et al., 1997; Ozaki et al., 1997), a subpopulation of renal epithelial cells that control renal excretion of base. IRR is also expressed in stomach enterochromaffin-like cells (Tsujimoto et al., 1995). These cells are located close to the stomach lining in the alkaline protective barrier and their function is to secrete histamine, a paracrine factor that modulates gastric acid secretion. Importantly, acid secretion by the stomach is paralleled by a massive efflux of bicarbonate into the extracellular medium surrounding the stomach epithelium, a phenomenon also known as the alkaline tide phenomenon (Niv and Fraser, 2002). In the pancreas, IRR is found in pancreatic β cells (Ozaki, 1998) that can face the duct lumen containing pancreatic juice with typical pH 8.0–8.5 and regulate bicarbonate secretion from the duct cells as the function of extracellular pH (Bertelli and Bendayan, 2005). Yet, in the nervous tissue cells, where IRR coexpresses with TrkA, its close chromosome neighbor sharing regulatory elements (Ma et al., 2000), extracellular pH reportedly cannot exceed 7.8 (Chesler, 2003) that would prevent IRR from activation. Therefore, its gene proximity-driven coexpression with TrkA may be either serendipitous or rudimentary that has not been eliminated by the evolutionary pressure.

As noted above, IRR is primarily expressed in kidney β IC cells that mediate net base secretion (or acid absorption) in response

to an alkali load, or to metabolic alkalosis. β IC cells are characterized by the presence of an apical Cl^-/HCO_3^- exchanger pendrin (pds, Slc26a4) and a basolateral vacuolar H^+-ATPase (Royaux et al., 2001). Another intercalated cell type, called α IC, exhibits the same acid-base transport properties but with the opposite polarization. Indeed, α IC cells harbor a basolateral Cl^-/HCO_3^- exchanger and an apical v-H^+-ATPase (Wall, 2005). As a consequence, α IC cells mediate net acid secretion (or base absorption). Depending on the conditions, the collecting duct can adapt rapidly from a state in which it does secrete acid, to another state in which it does secrete base (Schwartz et al., 1985). Importantly, it has been shown that exposure of isolated collecting duct to an acidic medium stimulates acid secretion and that the same tubule can revert its transport activity from proton to bicarbonate secretion if it is subsequently exposed to alkaline media (Purkerson et al., 2010). These studies indicate that intercalated cells are able to "sense" the pH of the extracellular fluid, and adapt their activity in the absence of any endocrine control.

We postulated that since IRR is a pH sensor activated by changes of extracellular pH toward alkaline value, it might be involved in the signaling pathway that triggers activation of bicarbonate secretion by IRR-expressing renal β IC cells in response to alkali loading. In support of this hypothesis, we found that IRR disruption impaired renal adaptation to alkali loading since $IRR^{-/-}$ mice developed metabolic alkalosis in response to this challenge. Moreover, this effect was related to the inability to increase pendrin expression, demonstrating that IRR is required for normal adaptation of the collecting duct to alkalosis.

EXPERIMENTAL PROCEDURES

Full-length cDNA clones of human IR, IGF-IR, and IRR were assembled from commercially available EST clones (I.M.A.G.E.) and fully verified by sequencing. Coding sequences of all receptor clones were in agreement with the corresponding GenPept entries with accession numbers AAA59452, AAP81165, and CAH70009. The cDNA clone of *Xenopus laevis* IRR was obtained from OpenBioSystem (clone ID 4031728). To generate HA epitope-tagged receptors, the receptor sequences were fused by PCR to the C-terminal nucleotide sequence encoding influenza hemagglutinin epitope tag (YPYDVPDYA) and subcloned into mammalian expression vector pcDNA3 (Invitrogen). Construction of IRR/IR mutants is described in the Supplement.

Transfections and Analysis of Receptor Tyrosine Kinase Activation in Cell Cultures

CHO cells were cultured in F-12 medium supplemented with 10% fetal bovine serum (Hyclone), 1% penicillin/streptomycin, and 2 mM L-glutamine. The COS, HEK293, HeLa, and A431 cells were cultured in DMEM supplemented with 10% fetal bovine serum (Hyclone), 1% penicillin/streptomycin, and 2 mM L-glutamine. MIN6 cells were cultured in DMEM supplemented with 10% fetal bovine serum (Hyclone), 1% penicillin/streptomycin, 2 mM L-glutamine, 0.11 mg/l pyruvate, and 30 μM β-mercaptoethanol.

CHO and HEK293 cells were transfected by unifectin-56 according to the manufacturer's protocol (Unifect Group, Russia). For selection of stably transfected clones, the cells were grown in the medium with added G418 antibiotic (Sigma, 600 μg/ml). Three independent IRR-overexpressing CHO cell lines were obtained with variable IRR expression but the same receptor properties with regards to the alkali stimulation.

In autophosphorylation assays, confluent monolayers of cells culture dishes were washed by serum-free F-12 and incubated overnight in serum-free F-12 containing 1% penicillin/streptomycin. The serum-starved cells were incubated with assayed media for 10 min at room temperature or at 37°C and solubilized in the lysis buffer (50 mM Tris-HCl [pH 7.5], 150 mM NaCl, 0.5% NP-40,

1% Triton X-100, 0.5 mM EDTA, 0.5 mM EGTA, 10% glycerol, 0.5 mM phenyl-methylsulphonyl fluoride, 1 mM Na_3VO_4, 1:100 [v/v] protease inhibitor cocktail [P8340, Sigma]) for 10 min on ice. Receptor tyrosine kinase activation was assessed by SDS-eletrophoresis of lysed cells or immunoprecipitates followed by western blotting and ECL detection by SuperSignal kits (Pierce), essentially as described (Krasnoperov et al., 2009; Deyev and Petrenko, 2010). The utilized antibodies are described in the Supplemental Experimental Procedures.

Activation of IRR in Intact Kidney under Alkali Load

The abdominal cavity of anesthetized rat was opened and a polyethylene (PE-50) catheter was implanted into the abdominal aorta via femoral artery so that the tip of catheter reached renal arteries. One percent $NaHCO_3$ solution was injected via catheter at a volume of 1 ml/100 g of body weight gradually, with 1 min intervals. A control animal was injected with appropriate volume of 0.9% NaCl. Urine was collected at 10 min intervals by urinary bladder syringe puncture and immediately transferred into vial for pH measuring with a microelectrode or test stripes. On reaching of urine pH >8.3, the kidneys were immediately excised and homogenized in 30 ml of 20 mM HEPES (pH 7.4), 10 mM EDTA, 3 mM Na_3VO_4, 1:100 (v/v) protease inhibitor cocktail (P8340, Sigma) in a glass-teflon homogenizer. The crude membrane fraction was obtained by centrifugation for 30 min at 30,000 g and extracted with 25 ml of 20 mM HEPES (pH 7.4), 150 mM NaCl, 1% Triton X-100, 10 mM EDTA, 3 mM Na_3VO_4, and 1:100 (v/v) protease inhibitor cocktail. The insoluble material was removed by centrifugation for 30 min at 50,000 g, and the obtained supernatant was filtered through 0.45 μm filter. IRR was immunoprecipitated with 8 μg purified anti-rIRR antibody or rabbit IgG (Imtek, Russia) from 6 ml extract and further analyzed by western blotting.

IRR Knockout Mice Analyses

$IRR^{-/-}$ mice were obtained by fertilization of C57BL6 wild-type mice with frozen sperm of $IRR^{-/-}$, $IR^{-/+}$, $IGF-IR^{-/+}$ mice (Nef et al., 2003). After more than eight cycles of breeding along with PCR genotyping, $IRR^{-/-}$ mice line of specific pathogen-free (SPF) status on a pure C57Bl6 genetic background was isolated.

All experiments were performed with age- and sex-matched $IRR^{-/-}$ and wild-type C57Bl6 mice (4 months old). Mice were given deionized water ad libitum, pair fed with standard laboratory chow containing 0.3% of sodium (INRA, France), and housed at constant room temperature (24°C ± 1°C) with 12 hr light/dark cycle. Urine collections were performed on mice kept in metabolic cages (Techniplast, France) in order to be able to verify accuracy of the pair feeding and to check that the volume of drinking solution was exactly identical between groups. Mice were first acclimatized for 4–5 days with a free access to deionized water and standard laboratory mice chow. Then experiments started at 9 a.m. after voiding the bladder by massage. Urine was collected by bladder massage at 3 p.m. (6 hr after the experiment started) and after 24 hr to measure pH and bicarbonate urinary excretion. On the second day, drinking water was replaced by 0.28 M $NaHCO_3$ solution and collections were repeated with the exactly same timing. This treatment has been shown previously by us to induce a mild metabolic alkalosis and to stimulate renal bicarbonate excretion in rats (Eladari et al., 2002; Quentin et al., 2004b), and the same effects have been described in mice by others (Wagner et al., 2002). Urine was collected under mineral oil to avoid CO_2 evaporation, and samples were analyzed immediately.

So that the chronic effects of alkaline loading on acid-base status of the animals could be tested, awake untreated mice were first sampled by retro-orbital puncture and blood gas was analyzed, then mice were allowed to recover during 2 weeks before starting alkaline loading with 0.28 M $NaHCO_3$ drinking solution. For confirmation that the effects observed after $NaHCO_3$ loading did not result from the sodium load, a control group consisted of $IRR^{-/-}$ or wild-type mice that were given 0.28 M NaCl drinking solution instead of 0.28 M $NaHCO_3$. After 7 days of loading, the mice were sampled and blood gas was analyzed again. Then mice were sacrificed and kidneys were removed for western blot analyses of pendrin and Atp6v1b1 protein abundance. Urine and blood pH and bicarbonate concentration were measured using a pH/blood gas analyzer (ABL 725, Radiometer, Copenhagen, Denmark).

REFERENCES

Bates, C.M., Merenmies, J.M., Kelly-Spratt, K.S., and Parada, L.F. (1997). Insulin receptor-related receptor expression in non-A intercalated cells in the kidney. Kidney Int. *52*, 674–681.

Bertelli, E., and Bendayan, M. (2005). Association between endocrine pancreas and ductal system. More than an epiphenomenon of endocrine differentiation and development? J. Histochem. Cytochem. *53*, 1071–1086.

Chesler, M. (2003). Regulation and modulation of pH in the brain. Physiol. Rev. *83*, 1183–1221.

Dandekar, A.A., Wallach, B.J., Barthel, A., and Roth, R.A. (1998). Comparison of the signaling abilities of the cytoplasmic domains of the insulin receptor and the insulin receptor-related receptor in 3T3-L1 adipocytes. Endocrinology *139*, 3578–3584.

De Meyts, P. (2002). Insulin and insulin-like growth factors: the paradox of signaling specificity. Growth Horm. IGF Res. *12*, 81–83.

De Meyts, P. (2008). The insulin receptor: a prototype for dimeric, allosteric membrane receptors? Trends Biochem. Sci. *33*, 376–384.

Deyev, I.E., and Petrenko, A.G. (2010). Regulation of CIRL-1 proteolysis and trafficking. Biochimie *92*, 418–422.

Dissen, G.A., Garcia-Rudaz, C., Tapia, V., Parada, L.F., Hsu, S.Y., and Ojeda, S.R. (2005). Expression of the insulin receptor-related receptor is induced by the preovulatory surge of luteinizing hormone in thecal-interstitial cells of the rat ovary. Endocrinology *147*, 155–165.

Dupont, J., and LeRoith, D. (2001). Insulin and insulin-like growth factor I receptors: similarities and differences in signal transduction. Horm. Res. *55* (*Suppl 2*), 22–26.

Eladari, D., Leviel, F., Pezy, F., Paillard, M., and Chambrey, R. (2002). Rat proximal NHE3 adapts to chronic acid-base disorders but not to chronic changes in dietary NaCl intake. Am. J. Physiol. Renal Physiol. *282*, F835–F843.

Flörke, R.R., Schnaith, K., Passlack, W., Wichert, M., Kuehn, L., Fabry, M., Federwisch, M., and Reinauer, H. (2001). Hormone-triggered conformational changes within the insulin-receptor ectodomain: requirement for transmembrane anchors. Biochem. J. *360*, 189–198.

Hernández-Sánchez, C., Mansilla, A., de Pablo, F., and Zardoya, R. (2008). Evolution of the insulin receptor family and receptor isoform expression in vertebrates. Mol. Biol. Evol. *25*, 1043–1053.

Hirayama, I., Tamemoto, H., Yokota, H., Kubo, S.K., Wang, J., Kuwano, H., Nagamachi, Y., Takeuchi, T., and Izumi, T. (1999). Insulin receptor-related receptor is expressed in pancreatic beta-cells and stimulates tyrosine phosphorylation of insulin receptor substrate-1 and -2. Diabetes 48, 1237–1244.

Jui, H.Y., Suzuki, Y., Accili, D., and Taylor, S.I. (1994). Expression of a cDNA encoding the human insulin receptor-related receptor. J. Biol. Chem. 269, 22446–22452.

Kanzaki, M. (2006). Insulin receptor signals regulating GLUT4 translocation and actin dynamics. Endocr. J. 53, 267–293.

Kelly-Spratt, K.S., Klesse, L.J., Merenmies, J., and Parada, L.F. (1999). A TrkB/insulin receptor-related receptor chimeric receptor induces PC12 cell differentiation and exhibits prolonged activation of mitogen-activated protein kinase. Cell Growth Differ. 10, 805–812.

Kelly-Spratt, K.S., Klesse, L.J., and Parada, L.F. (2002). BDNF activated TrkB/IRR receptor chimera promotes survival of sympathetic neurons through Ras and PI-3 kinase signaling. J. Neurosci. Res. 69, 151–159.

Kitamura, T., Kido, Y., Nef, S., Merenmies, J., Parada, L.F., and Accili, D. (2001). Preserved pancreatic beta-cell development and function in mice lacking the insulin receptor-related receptor. Mol. Cell. Biol. 21, 5624–5630.

Klammt, J., Garten, A., Barnikol-Oettler, A., Beck-Sickinger, A.G., and Kiess, W. (2005). Comparative analysis of the signaling capabilities of the insulin receptor-related receptor. Biochem. Biophys. Res. Commun. 327, 557–564.

Krasnoperov, V., Deyev, I.E., Serova, O.V., Xu, C., Lu, Y., Buryanovsky, L., Gabibov, A.G., Neubert, T.A., and Petrenko, A.G. (2009). Dissociation of the subunits of the calcium-independent receptor of alpha-latrotoxin as a result of two-step proteolysis. Biochemistry 34, 747–753.

Kristensen, C., Wiberg, F.C., and Andersen, A.S. (1999). Specificity of insulin and insulin-like growth factor I receptors investigated using chimeric mini-receptors. Role of C-terminal of receptor alpha subunit. J. Biol. Chem. 274, 37351–37356.

Lawrence, M.C., McKern, N.M., and Ward, C.W. (2007). Insulin receptor structure and its implications for the IGF-1 receptor. Curr. Opin. Struct. Biol. 17, 699–705.

Lou, M., Garrett, T.P., McKern, N.M., Hoyne, P.A., Epa, V.C., Bentley, J.D., Lovrecz, G.O., Cosgrove, L.J., Frenkel, M.J., and Ward, C.W. (2006). The first three domains of the insulin receptor differ structurally from the insulin-like growth factor 1 receptor in the regions governing ligand specificity. Proc. Natl. Acad. Sci. USA 103, 12429–12434.

Ma, L., Merenmies, J., and Parada, L.F. (2000). Molecular characterization of the TrkA/NGF receptor minimal enhancer reveals regulation by multiple cis elements to drive embryonic neuron expression. Development 127, 3777–3788.

Mathi, S.K., Chan, J., and Watt, V.M. (1995). Insulin receptor-related receptor messenger ribonucleic acid: quantitative distribution and localization to subpopulations of epithelial cells in stomach and kidney. Endocrinology 136, 4125–4132.

McKern, N.M., Lawrence, M.C., Streltsov, V.A., Lou, M.Z., Adams, T.E., Lovrecz, G.O., Elleman, T.C., Richards, K.M., Bentley, J.D., Pilling, P.A., et al. (2006). Structure of the insulin receptor ectodomain reveals a folded-over conformation. Nature 443, 218–221.

Nef, S., Verma-Kurvari, S., Merenmies, J., Vassalli, J.D., Efstratiadis, A., Accili, D., and Parada, L.F. (2003). Testis determination requires insulin receptor family function in mice. Nature 426, 291–295.

Niemeyer, M.I., González-Nilo, F.D., Zúñiga, L., González, W., Cid, L.P., and Sepúlveda, F.V. (2007). Neutralization of a single arginine residue gates open a two-pore domain, alkali-activated K+ channel. Proc. Natl. Acad. Sci. USA 104, 666–671.

Niv, Y., and Fraser, G.M. (2002). The alkaline tide phenomenon. J. Clin. Gastroenterol. 35, 5–8.

Ozaki, K. (1998). Insulin receptor-related receptor in rat islets of Langerhans. Eur. J. Endocrinol. 139, 244–247.

Ozaki, K., Takada, N., Tsujimoto, K., Tsuji, N., Kawamura, T., Muso, E., Ohta, M., and Itoh, N. (1997). Localization of insulin receptor-related receptor in the rat kidney. Kidney Int. 52, 694–698.

Purkerson, J.M., Tsuruoka, S., Suter, D.Z., Nakamori, A., and Schwartz, G.J. (2010). Adaptation to metabolic acidosis and its recovery are associated with changes in anion exchanger distribution and expression in the cortical collecting duct. Kidney Int. 78, 993–1005.

Quentin, F., Chambrey, R., Trinh-Trang-Tan, M.M., Fysekidis, M., Cambillau, M., Paillard, M., Aronson, P.S., and Eladari, D. (2004a). The Cl-/HCO3-exchanger pendrin in the rat kidney is regulated in response to chronic alterations in chloride balance. Am. J. Physiol. Renal Physiol. 287, F1179–F1188.

Quentin, F., Eladari, D., Frische, S., Cambillau, M., Nielsen, S., Alper, S.L., Paillard, M., and Chambrey, R. (2004b). Regulation of the Cl-/HCO3-exchanger AE2 in rat thick ascending limb of Henle's loop in response to changes in acid-base and sodium balance. J. Am. Soc. Nephrol. 15, 2988–2997.

Rentería, M.E., Gandhi, N.S., Vinuesa, P., Helmerhorst, E., and Mancera, R.L. (2008). A comparative structural bioinformatics analysis of the insulin receptor family ectodomain based on phylogenetic information. PLoS ONE 3, e3667.

Royaux, I.E., Wall, S.M., Karniski, L.P., Everett, L.A., Suzuki, K., Knepper, M.A., and Green, E.D. (2001). Pendrin, encoded by the Pendred syndrome gene, resides in the apical region of renal intercalated cells and mediates bicarbonate secretion. Proc. Natl. Acad. Sci. USA 98, 4221–4226.

Sabolić, I., Brown, D., Gluck, S.L., and Alper, S.L. (1997). Regulation of AE1 anion exchanger and H(+)-ATPase in rat cortex by acute metabolic acidosis and alkalosis. Kidney Int. 51, 125–137.

Schwartz, G.J., Barasch, J., and Al-Awqati, Q. (1985). Plasticity of functional epithelial polarity. Nature 318, 368–371.

Shier, P., and Watt, V.M. (1989). Primary structure of a putative receptor for a ligand of the insulin family. J. Biol. Chem. 264, 14605–14608.

Sparrow, L.G., McKern, N.M., Gorman, J.J., Strike, P.M., Robinson, C.P., Bentley, J.D., and Ward, C.W. (1997). The disulfide bonds in the C-terminal domains of the human insulin receptor ectodomain. J. Biol. Chem. 272, 29460–29467.

Srivastava, J., Barber, D.L., and Jacobson, M.P. (2007). Intracellular pH sensors: design principles and functional significance. Physiology 22, 30–39.

Tsujimoto, K., Tsuji, N., Ozaki, K., Ohta, M., and Itoh, N. (1995). Insulin receptor-related receptor messenger ribonucleic acid in the stomach is focally expressed in the enterochromaffin-like cells. Endocrinology 136, 558–561.

Ullrich, A., Bell, J.R., Chen, E.Y., Herrera, R., Petruzzelli, L.M., Dull, T.J., Gray, A., Coussens, L., Liao, Y.C., Tsubokawa, M., et al. (1985). Human insulin receptor and its relationship to the tyrosine kinase family of oncogenes. Nature 313, 756–761.

Ullrich, A., Gray, A., Tam, A.W., Yang-Feng, T., Tsubokawa, M., Collins, C., Henzel, W., Le Bon, T., Kathuria, S., Chen, E., et al. (1986). Insulin-like growth factor I receptor primary structure: comparison with insulin receptor suggests structural determinants that define functional specificity. EMBO J. 5, 2503–2512.

Wagner, C.A., Finberg, K.E., Stehberger, P.A., Lifton, R.P., Giebisch, G.H., Aronson, P.S., and Geibel, J.P. (2002). Regulation of the expression of the Cl-/anion exchanger pendrin in mouse kidney by acid-base status. Kidney Int. 62, 2109–2117.

Wall, S.M. (2005). Recent advances in our understanding of intercalated cells. Curr. Opin. Nephrol. Hypertens. 14, 480–484.

Ward, C.W., Garrett, T.P., McKern, N.M., Lou, M., Cosgrove, L.J., Sparrow, L.G., Frenkel, M.J., Hoyne, P.A., Elleman, T.C., Adams, T.E., et al. (2001). The three dimensional structure of the type I insulin-like growth factor receptor. MP, Mol. Pathol. 54, 125–132.

Zhang, B., and Roth, R.A. (1992). The insulin receptor-related receptor. Tissue expression, ligand binding specificity, and signaling capabilities. J. Biol. Chem. 267, 18320–18328.